Available online at www.sciencedirect.com
SCIENCE DIRECT®
Applied Clay Science 26 (2004) 389–401
Applied CLAY Science
www.elsevier.com/locate/clay

Microfabric of fractured Boom Clay at depth: a case study of brittle–ductile transitional clay behaviour

B. Dehandschutter[a,*], S. Vandycke[b], M. Sintubin[a], N. Vandenberghe[c], P. Gaviglio[d], J.-P. Sizun[d], L. Wouters[e]

[a] *Structural Geology and Tectonics Group, Katholieke Universiteit Leuven, Redingenstraat 16, B-3000 Leuven, Belgium*
[b] *Géologie Fondamentale et Appliquée, Faculté Polytechnique de Mons, 9 rue de Houdain, B-7000 Mons, Belgium*
[c] *Laboratorium voor Stratigrafie, Katholieke Universiteit Leuven, Redingenstraat 16, B-3000 Leuven, Belgium*
[d] *EA 2642 Géosciences, Université de Franche-Comté, 16, route de Gray, F-25030 Besançon cédex, France*
[e] *ONDRAF/NIRAS, Kunstlaan 14, B-1210 Brussels, Belgium*

Received 15 March 2003; received in revised form 29 July 2003; accepted 15 September 2003
Available online 27 February 2004

Abstract

Recent Underground Research Facility (URF) gallery excavation works in the Boom Clay at 224 m below the surface revealed intense fracturing of this weak claystone. Large fault planes (meter-scale) and joints were observed during tunnelling and found to belong to the excavation-disturbed zone (EDZ). Samples taken from the new gallery have been investigated using scanning electron microscope (SEM) imagery and microstructural analysis. This revealed a brittle–ductile transitional behaviour of the mudstone sediment regarding deformation, implying dilatant shear and hybrid fractures in high strain zones and ductile, compacted plastic shear bands in the lower strain zones, following an elasto-plastic constitutive model. Microfabric analysis contributed in this way to a better understanding of clay behaviour and effective fracturing. This information is primordial for understanding the rheology of the clay and assessing the influence of fracturing on permeability, critical issues in radioactive waste management.

Keywords: SEM microscopy; Microfabric; Boom Clay; Dilatancy; Ductility

1. Introduction

Although fairly suitable for describing the basic concepts of 'wet' rock and soil mechanics, elasto-plastic constitutive models and critical state soil mechanics (see, e.g. Wood, 1990) did, to date, not receive much attention in case studies of natural geological examples. This paper provides such a case study, which results from a survey carried out during gallery excavation for expansion of the Underground Research Facility (URF) at Mol, Belgium. The gallery is located in the Boom Clay Formation (Rupelian age), at a depth of 224 m below surface, on the SCK•CEN nuclear research centre site. The research facility (underground lab) is built to study the clay's potential

* Corresponding author. Tel.: +32-16-32-64-59; fax: +32-16-32-64-01.
E-mail address: boris.dehandschutter@geo.kuleuven.ac.be (B. Dehandschutter).

0169-1317/$ - see front matter © 2004 Elsevier B.V. All rights reserved.
doi:10.1016/j.clay.2003.12.013

as a host-rock for a long-term repository of high-level radioactive waste. The circular N–S oriented gallery ('Connecting Gallery', 83 m long) was constructed by removing clay using a tunnel boring machine with a roadheader and subsequently pushing an open shield (diameter of 4.8 m) into the remaining clay. Behind the shield, a wedge-block system was used as lining to support the gallery walls. As such, an excavation rate of more than 2 m per day was achieved. This method has two consequences: first, it causes fast clay removal and due advance; second, the sidewalls are quickly supported, preventing further radial accommodation (convergence) of the clay massif. Thus, the only zone exposed to relatively long-time stress relief is the frontal plane (front, see, e.g. Fig. 1).

During the excavation, large fractures in the clay massif were observed, both faults and joints—from millimeter scale to several meters large blocks. Mapping and sampling the fractures allowed to show their distinct macroscopic and microscopic characteristics providing a reasonable interpretation of their rheology, origin and formation mechanism (Dehandschutter et al., 2002). The present paper focuses on the microfabric of the fracture zones and on the influence of the fractures on the physical properties of the clay massif. The fracture zones can be both brittle (dilatant) and ductile, can display extension as well as shear and range in dimension from meter to micrometer scale.

2. The Boom Clay formation

The Boom Clay Formation (Rupelian, Oligocene) crops out in the central part of Flanders (Belgium) and extends in subcrop over large parts of the North Sea basin (see, e.g. Vandenberghe et al., 1998 and references therein). The formation is about 100 m thick in the area of the URF, with its base at about 290 m below the surface. It weakly dips ($\sim 1^{\circ}$) to the northeast and is composed of rhythmically alternating silt- and clay-rich beds. A candidate for the geological disposal of radioactive waste, the Boom Clay has been in recent years the object of many detailed stratigraphical (Van Echelpoel and Weedon, 1990; Vandenberghe et al., 1997, 1998), and geochemical (Laenen, 1999; De Craen et al., 1999) studies. This unlithified mudstone is mainly composed of kaolinite and illite with minor amounts of smectite and chlorite (Vanden-

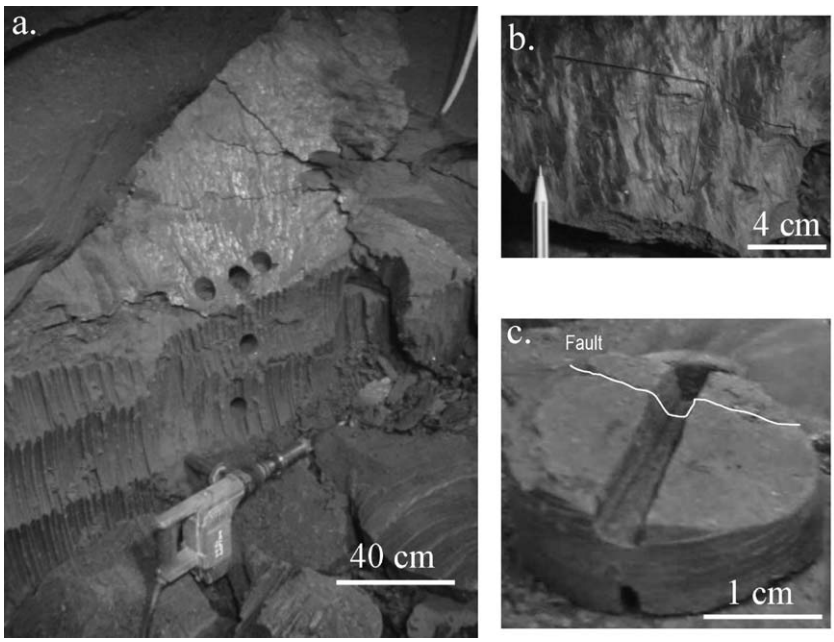

Fig. 1. (a) Example of a fault plane in the gallery front and oriented samples taken by a hand drill. (b) Slickenside showing shear direction and sense. (c) Prepared sample with precut seam allowing clean cut perpendicular to the fault.

berghe, 1978). It has a high water content of ~ 20% and a physical porosity of ~ 35%. The plastic clay is hardly overconsolidated (OCR ~ 1 to 1.5), with only minor uplift and erosion events recorded (Mertens et al., 2003). The angle of internal friction ϕ is around 10°, cohesion $c \sim 0.6$ MPa, Young modulus $E \sim 500$ MPa and Poisson ratio $\upsilon \sim 0.4$ (Schittekat et al., 1983; Arts, 2000). These properties classify the clay as a weak sediment.

3. Fracture characteristics

3.1. Natural versus artificial origin

Before the onset of tunnelling, doubt existed about the nature of the fractures, which where already noticed during vertical shaft excavation. In spite of the absence of any indications for the presence of faults during seismic reflection campaigns, the possible presence of preexisting fractures, consequently influencing the hydromechanical properties of the clay massif, had to be checked. Detailed fracture analysis showed that the majority of fractures encountered during gallery excavation has an artificial origin and belongs to the excavation-disturbed zone (EDZ). This conclusion is based on the geometry of the fractures, which is symmetric around the gallery axis, the kinematics (fault types) and dynamics (local stress state) responsible for the fracturing (Dehandschutter et al., 2002). The geometry of the local stress ellipsoid turned out to be dominated by stress concentration caused by the removal of the tunnelled clay and due to reorientation of the principal stress directions. These conclusions currently imply that no evidence is present that through-going fractures exist in the Boom Clay massif at the location of the URF, providing possible fracture porosities and potential fluid pathways. It was also shown that the vertical joint pattern observed in the (near surface) outcrop zone of the Boom Clay had little chance to extend in the deeper parts of the clay massif (Mertens et al., 2003).

3.2. Dilatancy versus compaction

The intensity of observed fractures and the surprisingly large volume of the collapsing blocks invoked questions about fracture mechanism and fracture microstructure that might affect the clay's physical properties (permeability, strength, anisotropy,...). Although artificially induced, these fractures could be important for the mechanical behaviour of the repository. To assess the role of the fractures in this matter, more knowledge about their nature is required. First of all, the rheological parameters and failure mechanism (brittle versus ductile, see Section 5.2) have to be qualified. Several authors describing failure in soft argillaceous sediments recognised millimeter-scale shear zones composed of parallel strands of reoriented clay particles ('scaly clays', Tchalenko, 1968; van den Berg, 1987; Agar et al., 1988; Arch et al., 1988). On the other hand, dilatant brittle fabrics also have been observed in weak mudrock (Ingram and Urai, 1999; Takizawa and Ogawa, 1999). The different responses of the same sediment are generally explained by its transition through several structural domains (depth ranges and/or tectonic stress changes). It is generally accepted that the overconsolidation ratio (OCR) governs the brittleness and hence the risk for dilatancy of unlithified argillaceous sediments (Jones and Addis, 1985; Ingram and Urai, 1999). Also, the water content and the strain rate control the deformation behaviour of clay (Arch et al., 1988). Are we, in the present case, dealing with open fractures, or are the faults sealed and closed? Why are both brittle and ductile structures observed on the same samples? Shear dilatancy versus pore collapse and compaction are important processes to consider in this matter, and their contribution to the failure of the Boom Clay in the URF is treated in this paper.

4. Experimental procedure

4.1. Sample preparation

Boom Clay material containing centimeter-scale slickensides (i.e. polished and striated fault planes, Fig. 1b) was sampled during gallery excavation, both from collapsed blocks at the open gallery front and from the sidewalls (Fig. 1a). Only at the first few meters of excavation oriented samples could be taken from the front because of collapse danger. Where possible, cylindrical oriented samples were taken using a slow rotating hand drill (Fig. 1a). The samples were cut to cubes or slices with two sides parallel to the

(subhorizontal) sedimentary bedding and two sides parallel to the movement direction (Fig. 1c). After precutting ditches were provided, the cubes were subjected to very slow drying in atmospheric conditions and subsequent controlled breaking parallel or perpendicular to the movement direction (Fig. 1c). This technique allows the observation of unaltered surfaces on samples as less disturbed as possible.

The process of drying could have had influence on the microporosity and microcracking because desiccation cracks tend to develop upon drying due to water evaporation and unequal swelling of the clay particles at the samples edge and more to its centre. That is why, for comparison, several samples have been investigated in undried ('wet') conditions using environmental SEM techniques, allowing for nonvacuum condition imaging of fresh samples. The same samples were subsequently dried and subjected to conventional SEM analyses. These tests showed that, when dried slowly enough (1–2 weeks) under atmospheric conditions, the differences between the 'wet' and the 'dry' samples regarding microcracking were negligible.

4.2. Porosimetry

Porosity and pore-size distribution of undisturbed Boom Clay were measured on slowly air-dried cylindrical samples (3 × 5 cm) by mercury injection. Injection results need to be interpreted cautiously, as applying the technique to soft rocks is ambiguous (Schlömer and Krooss, 1997). Sample drying and injecting mercury under pressure influences the clay's microstructure to certain extent, and the accessibility of small and isolated pores affects the measurement results. The obtained Hg porosity therefore only represents the porosity accessible for mercury, which is used here as an estimation determining the order of magnitude of the effective porosity.

5. Results and discussion

5.1. Microstructure observations

5.1.1. Preferred orientation of clay minerals

SEM (in secondary electron mode) images of all investigated Boom Clay samples show a well-developed preferred alignment of the clay particles parallel

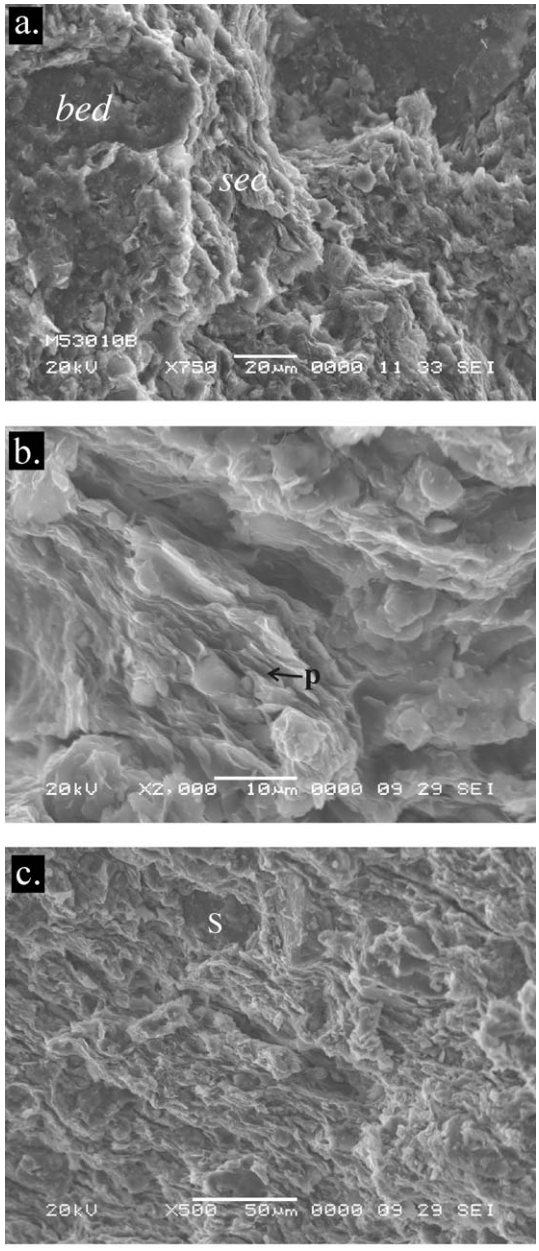

Fig. 2. SEM images of undisturbed Boom clay structure. (a) View on the bedding plane (*bed*) and on a section perpendicular (*sec*). (b) View on section perpendicular to the bedding, with interstitial pores (p). (c) View perpendicular to the bedding, showing clay particles warped around silt grain (s).

to the bedding surface (Fig. 2). This bedding shows a distinct porosity of the larger pores, caused by the granulometry (presence of silt particles) and the irregularity of the individual clay particles (Fig. 2b). In general, an open structure was observed with a high porosity. No flocculation was seen, and clay particles tend to wrap around silt particles (Fig. 2c). This indicates compaction corresponding to the slightly overconsolidated nature of the clay. Fig. 3 and Table 1 show the pore-size distribution obtained by mercury porosimetry of two representative samples. It shows that the majority of the pores has radii in the order of 0.01 μm. The connected porosity (reachable by mercury) lays around 28%. The images and the Hg porosity show that the (nondeformed) Boom Clay is an uncemented fine-grained compacted mud with a well-developed particle alignment (bedding) and a high porosity. The (subhorizontal) bedding is used as a reference anisotropy to distinguish deformation bands in the following sections.

5.1.2. Dilatancy by bedding activation

A type of dilatancy observed in several samples is presented in Fig. 4, where bedding planes oblique to the fault plane are activated and dilate. As such, fracture porosity is created. The amount of displacement by this mechanism is in the order of tenths of millimeters. This type of failure occurred in several fault blocks coming from the excavation front at different levels and therefore is supposed to exist over the whole extend of the gallery. It is not excluded that those fractures are connected to the main fault plane by secondary, oblique shear planes, undergoing even less displacement in the order of micrometers (Fig. 4b).

5.1.3. Dilatancy by Riedel Shear and en-echelon tension

During brittle faulting, secondary Riedel Shears develop at a small angle to the movement direction. These planes move (millimeter order of displacement) in the same sense as the (centimeter-scale displaced) master-plane (Fig. 5a and b). Along the Riedel planes, dilatancy occurs through pull-apart by fault drag in the movement sense (Fig. 5b). A detailed view of the relation between the bedding and the Riedel shear planes (Fig. 5c) shows how the clay particles are reoriented between the shear planes under micrometric scale shear. Note that only the major Riedel planes

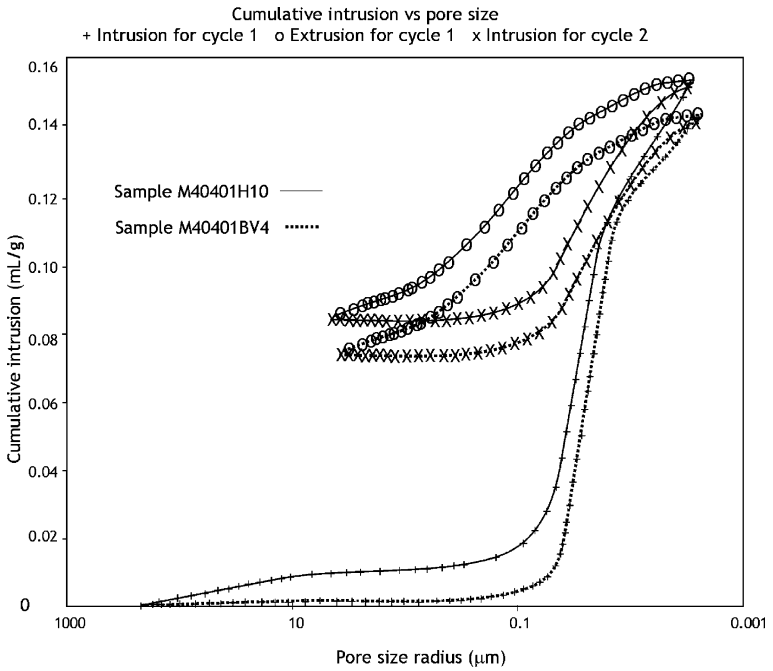

Fig. 3. Cumulative mercury intrusion versus pore size for undisturbed (not fractured) Boom Clay.

Table 1
Pore parameters and porosity deduced from Hg injection porosimetry

Sample	Results	
M40401H10	total intrusion volume	0.1525 ml/g
	total pore area	18.150 m^2/g
	median pore radius (volume)	0.0275 μm
	median pore radius (area)	0.0099 μm
	average pore radius (2*V*/*A*)	0.0168 μm
	bulk density at 0.0007 MPa	1.8842 g/ml
	apparent (skeletal) density	2.6441 g/ml
	porosity	28.74%
	stem volume used	35%
	threshold pressure	0.0136 MPa (calc.)
	characteristic length	45.7401 μm
M404001BV4	total intrusion volume	0.1608 ml/g
	total pore area	20.877 m^2/g
	median pore radius (volume)	0.0238 μm
	median pore radius (Area)	0.0106 μm
	average pore radius (2*V*/*A*)	0.0154 μm
	bulk density at 0.0007 MPa	1.8112 g/ml
	apparent (skeletal) density	2.5551 g/ml
	porosity	29.1156%
	stem volume used	53%
	threshold pressure	0.0528 MPa (calc.)
	characteristic length	11.8128 μm

(Fig. 5b) display dilatancy, whereas the minor planes (Fig. 5c) remain tight (see further).

In several places, en-echelon tension gashes adjoining normal faults are observed. Generally, they are oriented oblique to the bedding plane. Their (micrometric to millimetric) opening is perpendicular to the shortening direction (Fig. 6). This type of failure occurs mainly in the vicinity of high-strain normal faults.

Fig. 7 gives an example of bedding dilatancy, the strength of which was high enough to fracture a pyrite core. Although pure bedding dilatancy can be a result of drying (desiccation) the clay sample, comparison between 'wet' microscopy (environmental SEM, atmospheric conditions) and 'dry' (normal SEM, vacuum conditions) showed the occurrence of this type of dilatancy in both circumstances. Therefore, these structures are believed to result from the original clay deformation during failure.

5.1.4. Diffuse deformation in anastomosing shear bands

Apart from the evidences for brittle dilatancy, the investigated samples showed several zones with clear ductile deformation features. Most apparent are scaly fabrics (Maltman, 1987; Agar et al., 1988). They occur as parallel, anastomosing surfaces of compacted

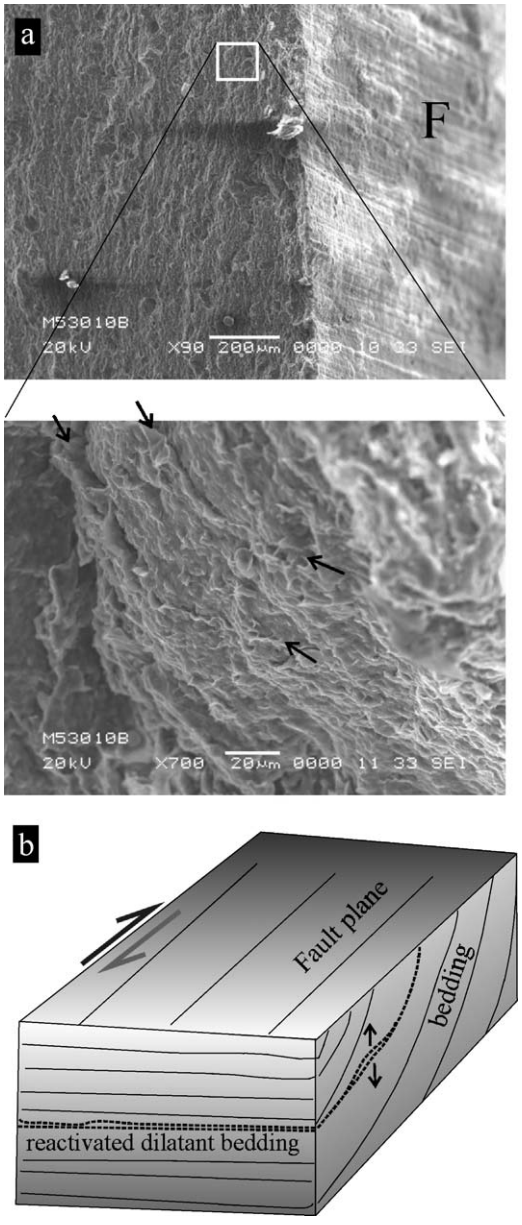

Fig. 4. (a) Example of dilatant bedding activation (arrows) in the vicinity of a normal fault slickenside (F). Movement is sinistral in the picture orientation, the missing block moving away from the viewer. (b) Possible connection between dilatant sheared bedding and controlling fault plane.

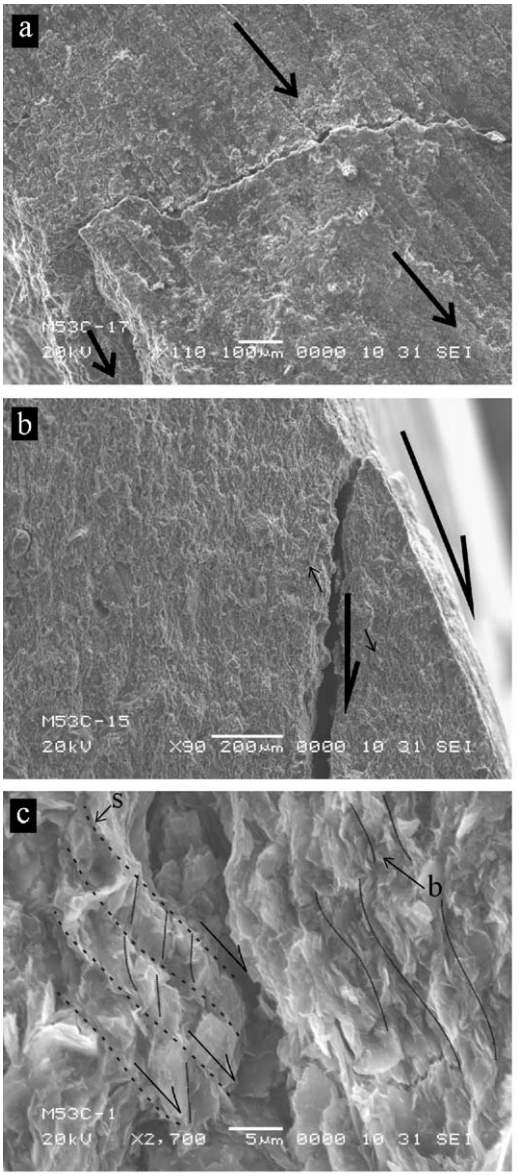

Fig. 5. (a) Normal fault plane with secondary Riedel shear. Arrows indicate movement of the missing block (hanging wall). (b) Perpendicular view showing dilatancy (small full arrows) along Riedel shear plane having the same displacement as the main plane (indicated by the larger half arrows). (c). Close-up of figure (b), showing the relation between bedding (b) and Riedel shear planes (s). The bedding is reoriented by slip along the shear planes.

and aligned (reoriented) clay particles inside which a porosity reduction can be supposed. Fig. 8 gives an example of such ductile shear zones. Compared with the brittle expressions of fracturing, ductile deformation was rarely observed. On the contrary, samples taken from Boom Clay at the surface in outcrops often display ductile deformation (work in progress, Dehandschutter et al., 2003).

One of the few forms in which ductile shear deformation has been observed are listric secondary (micrometer-scale) shear zones oblique to the main movement plane (Fig. 9). The ductile zones occur as micrometric strands with a strong reorientation and compaction of the clay particles.

5.1.5. Fault tips in ductile compaction settings

Ductile shear bands with particle displacements (rotations) of a few micrometers are observed at fault tips, where strain dies out. Clay particles are reoriented and aligned perpendicular to the principal

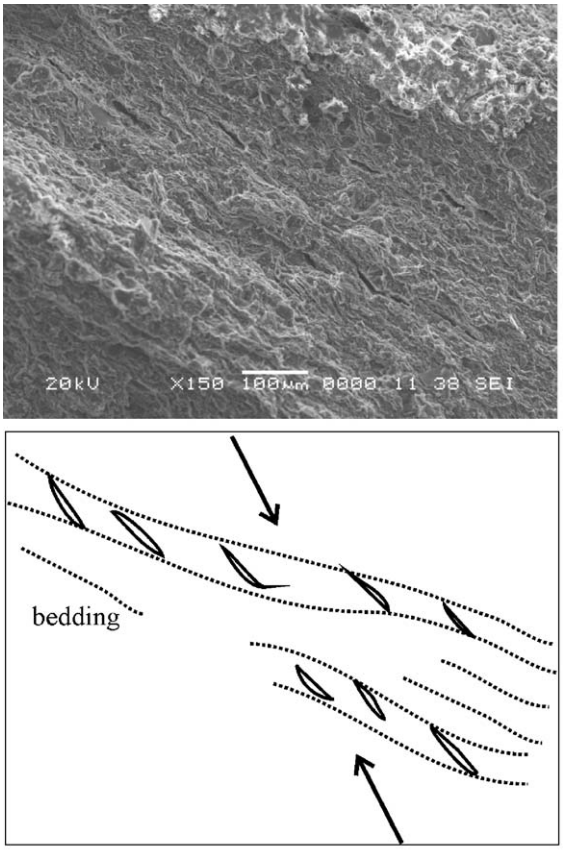

Fig. 6. Example of en-echelon tension gashes opening oblique to the bedding plane, perpendicular to the shortening direction (arrows).

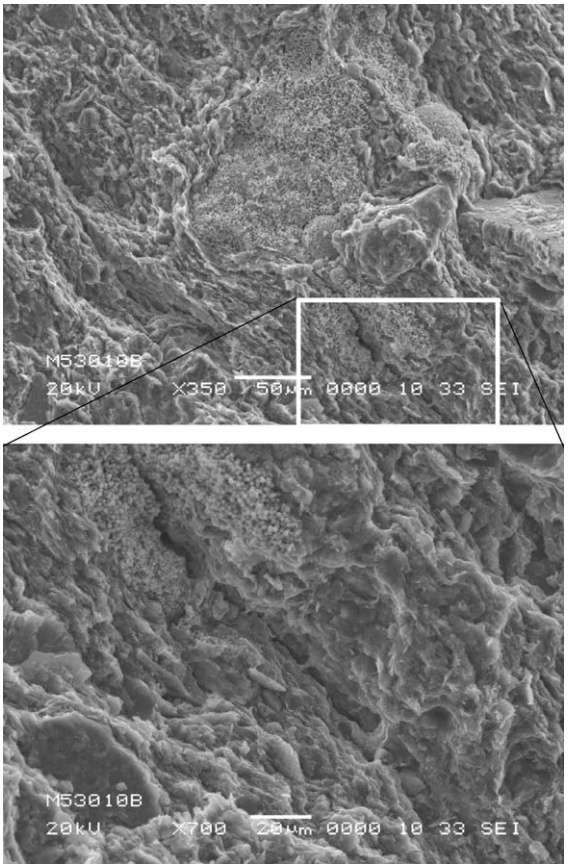

Fig. 7. Bedding dilatancy fracturing of a pyrite core.

shortening direction without the loss of cohesion (Fig. 10). In this way, the tips of the dilatant fault planes end in nondilatant ductile shear bands. They are indicative for porosity loss through compactive pore collapse.

5.2. Deformation mechanism and clay rheology

Physically, clay and mud are transitional between rock and soil, and therefore argillaceous material exhibits a mechanically transitional behaviour. In addition, muds are transitional in time and tend to transgress from rock-like behaviour to soil-like behaviour within a relatively short time period (Jones and Addis, 1986). Various experiments showed that clay deforms by brittle failure at low mean effective stresses and by ductile shear at high mean effective stresses (Bishop et al., 1965; Horseman et al., 1996). Water content also influences the clay behaviour, the latter getting more ductile with increasing water content (Arch et al., 1988). Distinction between brittle and ductile behaviour is based on the shear stress–shear strain relation (Fig. 11). If distinct peak strength is followed by strong strain weakening (failure) during progressive shear strain, we define the deformation as brittle. If peak strength is undefined, elasticity is weak (low Young modulus) and strain hardening dominates, failure is called ductile (Fig. 11).

Several experimental studies report the development of ductile shear bands in clay during deformational experiments (Tchalenko, 1968; van den Berg, 1987; Arch et al., 1988). Scaly fabrics observed in different mudstones showed a variety of microfabric geometry (plastic and dilatant), ascribed to different structural (and mean effective stress) levels of the different clays and to changes in pore-fluid pressure and strain rate (Agar et al., 1988; Takizawa and Ogawa, 1999). The deformation of the Boom Clay can be described by an elasto-plastic constitutive model to explain the coexistence of brittle and ductile fabrics, based on amount of shear strain, where shear strain is concentrated along both ductile (non-dilatant) and brittle (dilatant) shear bands.

5.3. Elasto-plastic deformation of the Boom Clay

A general observation made about the microfabric of the disturbed zones along the whole excavated gallery is the coexistence of both brittle and ductile

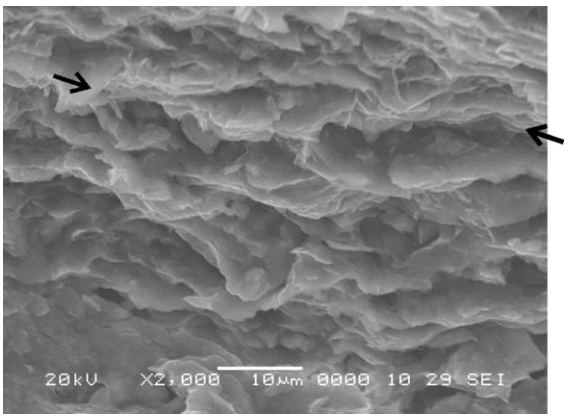

Fig. 8. Example of ductile shear bands in the Boom Clay at the URF (between arrows).

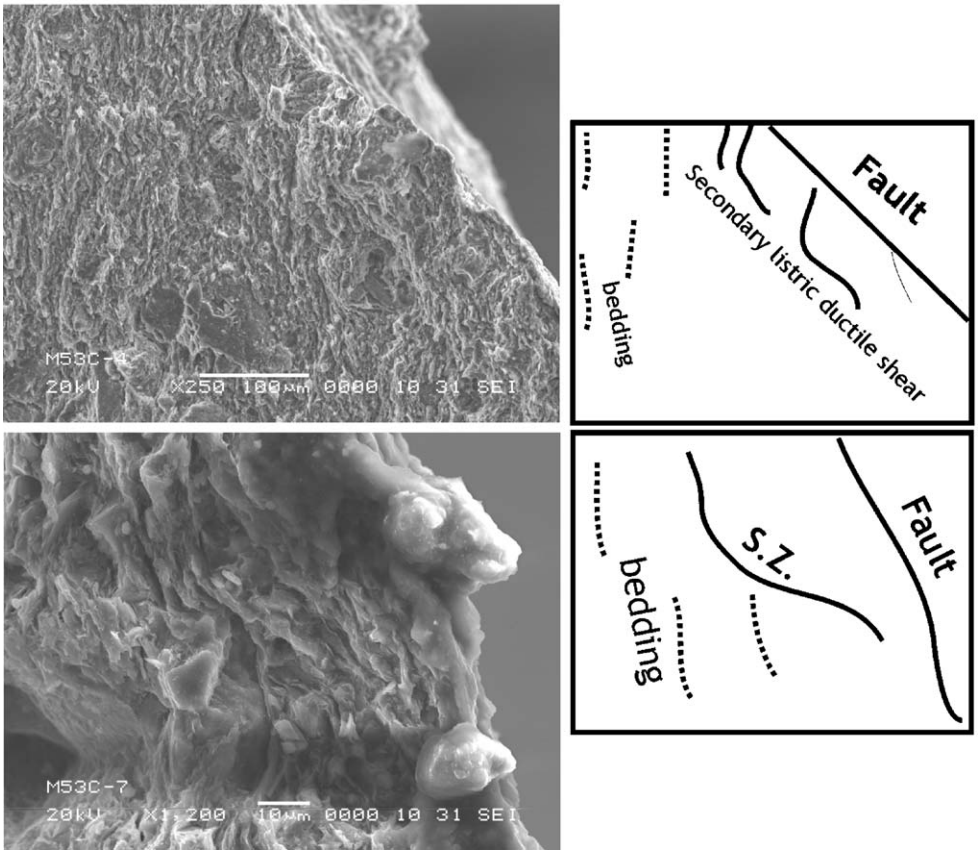

Fig. 9. Examples of ductile shear bands occurring as compacted secondary listric faults.

structures in the same leading fault zones. Fig. 12 illustrates the stress situation of the Boom Clay at the URF at Mol at different time points in Mohr–Coulomb space. Stress circle 1 shows the initial stress situation corresponding to a vertical σ_1 and a horizontal σ_3 deduced from a k_0 value of 0.8 (Horseman et al., 1993). Total vertical stress is 4.6 MPa, and assuming a hydrostatic pore pressure of 2.2 MPa, effective vertical stress is 2.4 MPa and effective horizontal stress is around 1.9 MPa. The differential stress is thus 0.25 MPa at a mean effective stress of 2.15 MPa. This stress condition is clearly unfavourable for brittle failure. However, due to the void created by the horizontally excavated gallery, the horizontal (axial) stress (σ_3) drops at the (unsupported) gallery front, whereas the vertical stress reduces much less at the gallery front due to fast sidewall support (Fig. 12, circle 2). This has a consequence that the Mohr–Coulomb failure criterion is passed and failure can occur on planes favourably oriented relative to the maximal compression direction. Because this direction changes in function of the position in the gallery (close to the centre or close to the front), a variety of slip planes will develop (Dehandschutter et al., 2002). As a result of gallery excavation, the least principal stress will drop towards zero, virtually creating conditions of high differential stress-inducing shear faults (Fig. 12, circle 3). Effective normal stress is now sufficiently low for brittle and hybrid shear fractures to develop (Engelder, 1994).

Dealing with soft sediment deformation, we have to consider volumetric strain and plastic transitional behaviour of the clay (Maltman, 1994; Petley, 1999). Fig. 13 proposes a schematic diagram of the (elasto-plastic) stress path followed by the Boom Clay during the excavation of the gallery to explain the develop-

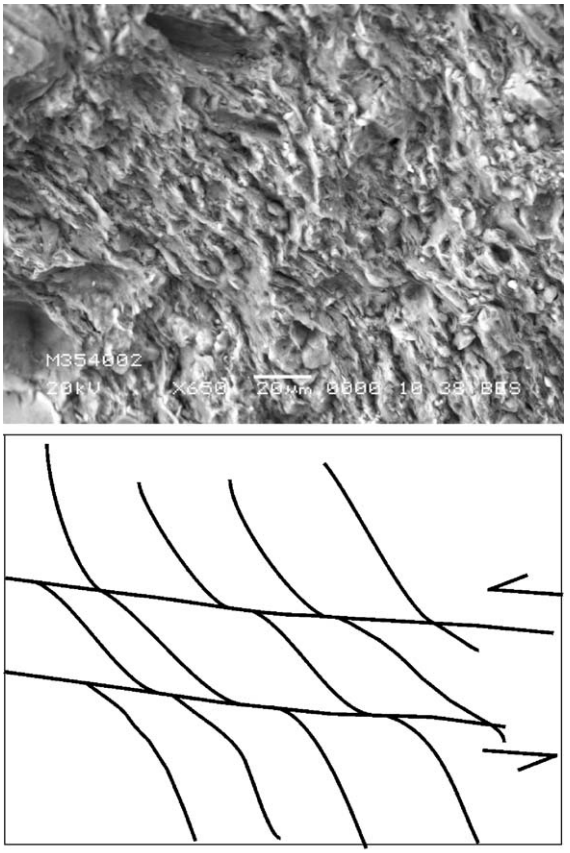

Fig. 10. Ductile shear zone developing at the fault tip where shear strain extincts. Deformation is accommodated by a reorientation of the clay particles in sinistral simple-shear conditions, without loss of cohesion. The principal shortening direction here is upper-right–lower-left of the photograph.

ment of the different microstructures initiating at different stages during deformation. Some stages in the stress path are denoted by numbers:

(1) Early, burial-related consolidation along a k_0 stress path. Deformation occurs by volumetric strain (porosity reduction) and accentuates bedding anisotropy and clay particle alignment (Fig. 2).
(2) At the onset of excavation, differential stress is increased and mean effective stress reduced (by the opening of the gallery). The stress path follows the plastic yield surface and ductile deformation takes place in the low strain zones (Section 5.1, Figs. 5 and 8).

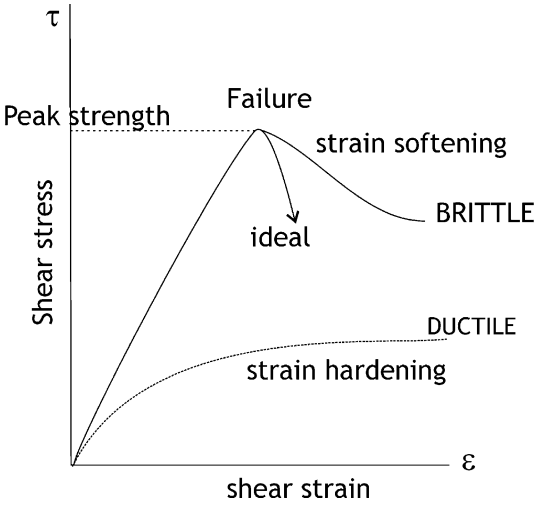

Fig. 11. Distinction between brittle and ductile failure in a shear stress–shear strain diagram.

(3) At a certain strain level, peak strength is reached and brittle faults with dilatancy develop (Section 5.1, Figs. 4–7), up to the residual strength envelope (4).
(4) At the clay's residual strength level, shear strain ceases and faults are blocked.

It is obvious that, depending on the convergence of the clay and hence on the support of the lining and the speed of excavation, strain can attain different amounts

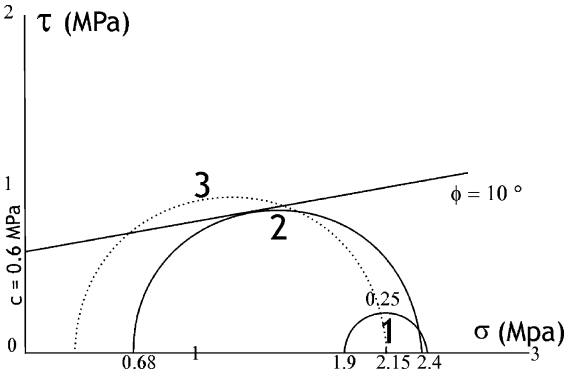

Fig. 12. Mohr–Coulomb diagram showing the various stress states for the Boom Clay before (circle 1) and during (circle 2) gallery excavation. Circle 3 shows the hypothetical circle for a total drop of sigma 3, indicating strong differential stress causing failure and intense faulting in the clay massif, in agreement with the observations.

in different adjoining zones of the same clay, allowing both ductile and brittle fabric to occur close to each other.

Fracture porosity and related fluid flow will occur only in case of dilatancy of the clay body, associated to shear strains under differential stress. In general, the onset of dilatancy is controlled by the critical state line and the critical state friction parameter M (Fig. 13, compressive strength/mean effective stress ratio, Ingram and Urai, 1999). As long as critical stress ratio is not reached, strain will be first volumetric for normally consolidated sediments, and later, when the plastic yield surface is reached, ductile. If the stress path passes the critical state line at peak strength, brittle failure will occur with resulting fracture porosity (e.g. Roscoe and Burland, 1968; Wood, 1990; see Fig. 13).

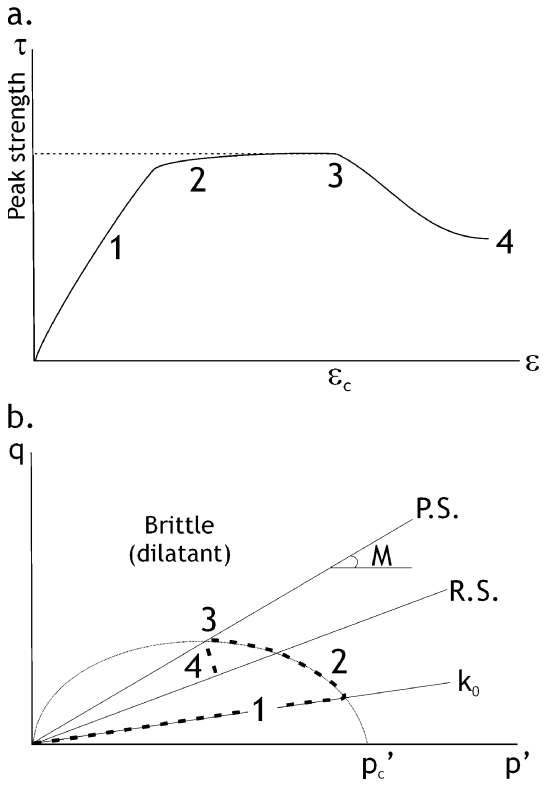

Fig. 13. Model for the deforming Boom Clay at the URF during gallery excavation. (a) Shear stress–shear strain diagram illustrating the concept of transitional clay behaviour. 1. k_0 strain path. Deformation by volumetric strain (void ratio reduction). 2. Plastic failure. 3. Brittle failure. 4. Residual strength. (b) Differential stress (q)–mean effective stress (p') diagram illustrating the possible effective stress path followed by the Boom Clay during deformation (dashed line). P.S.: peak strength. R.S.: residual strength. k_0: normal consolidation line.

6. Conclusions

The Boom Clay, deformed by stress concentration during gallery excavation at 224 m below the surface, shows a wide variety of microstructures (centimeter to micrometer scale), ranging from pure dilatant brittle faults and tension gashes to plastic and compacted ductile shear bands. Both types of shear zones occur very close to each other on the same hand-piece samples. It is clear that most of the dilatant (open) fractures are due to dynamic deformation and are not merely artefacts created by desiccation or decompression. The clay deformation described here provides a good example of brittle–ductile transitional behaviour in undrained conditions, mainly controlled by fracture orientation and shear strain, and changes in the local confining pressure. This is due to the nature of the deformation, caused by gallery excavation. Ductile, plastic deformation occurs in relatively low strain zones (micrometric displacements), where a reorientation of the clay particles together with a reduction of pore space along the shear zones determines the local fabric, which is closed. In high strain zones (centimetric displacements), affected by larger strain rates (block collapse), a brittle, dilatant fabric dominates. An explanation for the observed transitional fabric is found in the elasto-plastic constitutive model applicable for weak clays with high water content. After the plastic yield surface has been reached, ductile deformation takes place by compactive particle reorientation, up to the moment where shear strain attains a level where cohesion is lost and brittle, dilatant fractures (faults and joints) develop.

This study contributes to the understanding of transitional mudstone deformation by providing a microscopic morphological description of deformed mudstone, sampled at depth (224 m). Dilatancy, the process responsible for fracture porosity and permeability increase creating preferential pathways and possible fluid flow with increase in hydraulic conductivity in an otherwise impervious mudstone, is shown to be possibly caused by formation of large macro-

scopic dilatant shear fractures (faults and joints) and by microcracking prior to macroscopic failure (brittle dilatant response).

Acknowledgements

The present study is sponsored by ONDRAF/NIRAS (Belgian radioactive waste agency), in collaboration with K.U. Leuven (Belgium), Faculté Polytechnique (Mons, Belgium) and Université de Franche-Comté (Besançon, France). Manuel Sintubin is Research Associate of the Onderzoeksfonds K.U. Leuven (Belgium). Sara Vandycke is Chercheur Qualifié of the F.N.R.S. (Belgium). Thanks to Prof. Janos Urai (RWTH Aachen, Germany) for useful discussions on sample preparation techniques and clay rheology and to the anonymous reviewers for constructive comments on an earlier version of the manuscript. The authors thank SCK•CEN and E.I.G. EURIDICE for offering the possibility of a fracture study and sampling campaign during tunnel excavation and for the fruitful cooperation.

References

Agar, S.M., Prior, D.J., Behrmann, J.H., 1988. Back-scattered electron imagery of the tectonic fabrics of some fine-grained sediments: implications for fabric nomenclature and deformation processes. Geology 17, 901–904.

Arch, J., Maltman, A.J., Knipe, R.J., 1988. Shear-zone geometries in experimentally deformed clays: the influence of water content, strain rate and primary fabric. Journal of Structural Geology 10, 91–99.

Arts, R., 2000. Transport of radionuclides through a clay barrier. TNO-NITG, 8–11.

Bishop, A.W., Webb, D.L., Skinner, A.E., 1965. Triaxial tests on soil at elevated cell pressures. Proceedings of the International Conference on Soil Mechanics, Montreal, 170–174.

De Craen, M., Swennen, R., Keppens, E.M., Macauley, C.I., Kiriakoulakis, K., 1999. Bacterially mediated formation of carbonate concretions in the Oligocene Boom Clay of northern Belgium. Journal of Sedimentary Research (SEPM) 69, 1098 (abstract).

Dehandschutter, B., Sintubin, M., Vandenberghe, N., Vandycke, S., Gaviglio, P., Wouters, L., 2002. Fracture analysis in the Boom Clay (URF, Mol, Belgium). Aardkundige Mededelingen 12, 245–248.

Dehandschutter, B., Sintubin, M., Vandenberghe, N., Vandycke, S., Gaviglio, P., Wouters, L., 2003. Brittle–ductile behaviour of critically stressed unconsolidated argillaceous sediments. Naturally Fractured Rock Formations, International Francqui Chair Final Colloquium, Liège 2003. ULg, Liège. Abstract volume, 5 pp.

Engelder, T., 1994. Brittle crack propagation. In: Hancock, P.L. (Ed.), Continental Deformation. Pergamon, Oxford, pp. 43–52.

Horseman, S.T., Winter, M.G., Entwistle, D.C., 1993. Triaxial experiments on Boom Clay. In: Cripps, J.C., Coulthard, J.M., Culshaw, M.G., Forster, A., Hencher, S.R., Moon, C.F. (Eds.), The Engineering Geology of Weak Rock. Balkema, Rotterdam, pp. 36–43.

Horseman, S.T., McCann, D.M., McEwan, T.J., Brightman, M.A., 1996. Determination of the geotechnical properties of mudrock from geophysical logging of the Harwell boreholes. FLPU British Geological Survey. Fluid Processes Research Group. British Geological Survey, London, pp. 14–84.

Ingram, G.M., Urai, J.L., 1999. Top-seal leakage through faults and fractures: the role of mudrock properties. In: Aplin, A.C., Fleet, A.J., Macquaker, J.H.S. (Eds.), Muds and Mudstones: Physical and Fluid Flow Properties. Geological Society of London, Special Publication, vol. 158, pp. 125–135.

Jones, M.E., Addis, M.A., 1985. On the changes in porosity and volume during a burial of argillaceous sediments. Marine and Petroleum Geology 2, 247–252.

Jones, M.E., Addis, M.A., 1986. The application of stress path and critical state analysis to sediment deformation. Journal of Structural Geology 8, 575–580.

Laenen, B., 1999. The geochemical signature of relative sea-level cycles recognised in the Boom Clay. Aardkundige Mededelingen 9, 61–82.

Maltman, A.J., 1987. Microstructures in deformed sediments, Denbigh Moors, North Wales. Geological Journal 22, 87–94.

Maltman, A.J., 1994. Prelithification deformation. In: Hancock, P.L. (Ed.), Continental Deformation. Pergamon, Oxford, pp. 143–158.

Mertens, J., Vandenberghe, N., Wouters, L., Sintubin, M., 2003. The origin and development of joints in the Boom Clay Formation (Rupelian) in Belgium. In: Van Rensbergen, P., Hillis, R.R., Maltman, A.J., Morley, C.K. (Eds.), Subsurface Sediment Mobilization. Geological Society of London, Special Publication, vol. 217, pp. 311–323.

Petley, D.N., 1999. Failure envelope of mudrocks at high confining pressures. In: Aplin, A.C., Fleet, A.J., Macquaker, J.H.S. (Eds.), Muds and Mudstones: Physical and Fluid Flow Properties. Geological Society of London, Special Publication, vol. 158, pp. 61–71.

Roscoe, K.H., Burland, J.B., 1968. On the generalised stress–strain behaviour of 'wet' clay. In: Heyman, J., Leckie, F.A. (Eds.), Engineering Plasticity. Cambridge Univ. Press, Cambridge, pp. 535–609.

Schittekat, J., Henriet, J.P., Vandenberghe, N., 1983. Geology and geotechnique of the Scheldt Surge Barrier. Characteristics of an overconsolidated clay. 8th International Harbour Congress, vol. 2. Harbour Press, Antwerp, pp. 121–135.

Schlömer, S., Krooss, B.M., 1997. Experimental characterisation of the hydrocarbon sealing efficiency of cap rocks. Marine and Petroleum Geology 14, 565–580.

Takizawa, S., Ogawa, Y., 1999. Dilatant clayey microstructure in

the Barbados décollement zone. Journal of Structural Geology 21, 117–122.

Tchalenko, J.S., 1968. The evolution of kink-bands and the development of compression textures in sheared clays. Tectonophysics 6 (2), 159–174.

van den Berg, L., 1987. Experimental redeformation of naturally deformed scaly clays. Geologie en Mijnbouw 65, 309–315.

Vandenberghe, N., 1978. Sedimentology of the Boom Clay (Rupelian) in Belgium: Verhandeling Koninklijke Academie voor Wetenschappen, 147, Letteren en Schone Kunsten van België, Klasse der Wetenschappen, Brussel. 137 pp.

Vandenberghe, N., Laenen, B., Van Echelpoel, E., Lagrou, D., 1997. Cyclostratigraphy and climatic eustasy. Example of the Rupelian stratotype. Comptes Rendus de l'Académie des Sciences—Earth and Planetary Science 325, 305–315.

Vandenberghe, N., Laga, P., Steurbaut, E., Hardenbol, J., Vail, P., 1998. Tertiary sequence stratigraphy at the southern border of the North Sea Basin in Belgium. In: de Graciansky, P.C., Hardenbol, J., Jacquin, Th., Vail, P.R. (Eds.), Mesozoic and Cenozoic Sequence Stratigraphy of European Basins. SEPM Special Publication No. 60. SEMP, Tulsa, USA, pp. 119–154.

Van Echelpoel, E., Weedon, G.P., 1990. Milankovich cyclicity and the Boom Clay Formation: an Oligocene siliciclastic shelf sequence in Belgium. Geological Magazine 127, 599–604.

Wood, D.M., 1990. Soil Behaviour and Critical State Soil Mechanics. Cambridge Univ. Press, Cambridge. 462 pp.